Antitumor activity via apoptotic cell death pathway of water soluble copper(II) complexes: effect of the diamino unit on selectivity against lung cancer NCI-H460 cell line

Wagner da S. Terra · Érika S. Bull · Samila R. Morcelli · Rafaela R. Moreira ·
Leide Laura F. Maciel · João Carlos de A. Almeida · Milton M. Kanashiro ·
Christiane Fernandes · Adolfo Horn Jr

Abstract The cytotoxicity against five human tumor cell lines (THP-1, U937, Molt-4, Colo-205 and NCI-H460) of three water soluble copper(II) coordination compounds containing the ligands 3,3′-(ethane-1,2-diylbis(azanediyl))dipropanamide (BCEN), 3,3′-(piperazine-1,4-diyl)dipropanamide (BPAP) or 3,3′- and (1,4-diazepane-1,4-diyl)dipropanamide (BPAH) are reported in this work. The ligands contain different diamine units (ethylenediamine, piperazine or homopiperazine) and two propanamide units attached to the diamine centers, resulting in N_2O_2 donor sets. The complex containing homopiperazine unit presented the best antiproliferative effect and selectivity against lung cancer cell line NCI-H460, showing inhibitory concentration (IC_{50}) of 58 μmol dm^{-3} and Selectivity Index (SI) > 3.4. The mechanism of cell death promoted by the complex was investigated by Sub-G1 cell population analysis and annexin V and propidium iodide (PI) labeling techniques, suggesting that the complex promotes death by apoptosis.

W. da S. Terra · É. S. Bull · S. R. Morcelli ·
R. R. Moreira · C. Fernandes · A. Horn Jr (✉)
Laboratório de Ciências Químicas, Universidade Estadual
do Norte Fluminense Darcy Ribeiro,
Campos dos Goytacazes, RJ 28013-602, Brazil
e-mail: adolfo.junior@ufsc.br

W. da S. Terra · É. S. Bull
Instituto Federal Fluminense, Campos dos Goytacazes,
RJ 28030-130, Brazil

Present Address:
S. R. Morcelli
Secretaria de Educação do Espírito Santo,
Mimoso Do Sul, ES 29400-000, Brazil

Present Address:
R. R. Moreira
Centro Federal de Educação Tecnológica, Nova Friburgo,
RJ 28635-080, Brazil

L. L. F. Maciel · J. C. de A. Almeida
Laboratório de Fisiologia e Bioquímica de
Microrganismos, Universidade Estadual do Norte
Fluminense Darcy Ribeiro, Campos dos Goytacazes,
RJ 28013-602, Brazil

M. M. Kanashiro
Laboratório de Biologia do Reconhecer, Universidade
Estadual do Norte Fluminense Darcy Ribeiro,
Campos dos Goytacazes, RJ 28013-602, Brazil

Present Address:
C. Fernandes · A. Horn Jr
Departamento de Química, Universidade Federal de Santa
Catarina, Florianópolis, SC 88040-900, Brazil

Transmission electron microscopy investigations are in agreement with the results presented by mitochondrial membrane potential analysis and also show the impairment of other organelles, including endoplasmic reticulum.

Keywords Copper coordination compound · Tetradentate ligand · Cytotoxicity · Apoptosis · Cancer · Chemotherapy

Introduction

According to WHO, cancer is a chronic disease with an important impact on public health worldwide, accounting for around 15% of all causes of death in the world (*Cancer*, https://www.who.int/news-room/fact-sheets/detail/cancer). It is represented by a heterogeneous group of diseases that cause great fear in the society, by becoming a stigma of death and pain. Despite this fact, this set of diseases has as an unifying characteristic the creation of abnormal cells that grow beyond their natural limits in an uncontrolled way, disobeying the normal processes of cell division (Ahmad and Ahsan 2020; Gutschner and Diederichs 2012; Pugazhendhi et al. 2018).

The great diversity of human cell types makes possible a large number of cancer cells. Among these, lung cancer is one of the most common and malignant, representing 11.6% of all diagnoses and 18.4% of deaths related to this disease worldwide (Arffman et al. 2018; Bray et al. 2018; Huang et al. 2020). In addition, these rates for lung cancer are increasing year by year, becoming the most common type of cancer among men and the second most common among women, behind only breast cancer. Studies report that the 5-year survival rate of patients with lung cancer is less than 18%, while, in the case of advanced metastatic lung cancer, this value reduces to only 5% (Arffman et al. 2018; Cong et al. 2020; Riddell and Lippard 2018; Shi et al. 2019). The main risk factor for this type of cancer is smoking, but other factors such as genetic susceptibility, diet, vitamin supplements, physical activity and occupational and environmental exposures also need to be taken into account for the development of this disease (Huang et al. 2020; Bray et al. 2018). Given these data, the early and accurate pathological diagnosis and the appropriate treatment, becomes an important link to minimize mortality rates (Cong et al. 2020).

Nowadays, the main treatments for cancer involve surgery, radiation therapy, chemotherapy, targeted therapy, hormonal therapy and immunotherapy (Miller et al. 2019; Wang et al. 2019).

With regard to chemotherapy, the discovery of cisplatin's antitumor activity is a milestone for the medicinal inorganic chemistry (Muhammad and Guo 2014; Riddell and Lippard 2018). Since then, the goal in the development of new coordination compounds with such activity is a competitive topic that permeates different areas, including chemistry, biology, pharmacy and medicine. Such interest has been motivated by the side effects shown by cisplatin, the lack of effective activity on a number of tumor types as well as by the development of resistance (Adams et al. 2014; Florea and Büsselberg 2011; Gallagher et al. 1997; Kartalou and Essigmann 2001; Stewart 2007).

In this scenery, the synthesis of new coordination compounds with anticancer activity has been pursued and expanded to other metal ions (Ru, Ga, Ti, V) (Babak and Ang 2018; Chitambar 2018; Cini et al. 2017; Crans et al. 2018; Kioseoglou et al. 2015; Lessa et al. 2012; Tshuva and Miller 2018; Zeng et al. 2017) including those with essential functions in the human body as iron and copper (Borges et al. 2016; Denoyer et al. 2018; Santini et al. 2014; Wani et al. 2016).

Concerning to iron compounds, the formation of Fe(II)-bleomycin inside cells has resulted in a very effective chemotherapeutic whose action mode is related to the generation of reactive oxygen species that promote the DNA cleavage through oxidation (Yu et al. 2016). Compared to iron, copper has been a more profitable element concerning the development of antitumor compounds. In this regard, copper compounds containing elesclomol, thiosemicarbazones or phenantroline/bypiridine (Casiopeinas) as ligands have reached clinical trials (Denoyer et al. 2018; Ruiz-Azuara et al. 2014; Santini et al. 2014).

We have been evaluating the anticancer activity of a series of coordination compounds containing different metal ions both in vitro and in vivo as well (Borges et al. 2016; Fernandes et al. 2015, 2006; Horn Jr. et al. 2013; Morcelli et al. 2016a, b; Morcelli et al. 2016a, b; Moreira et al. 2019). Concerning in vitro studies, the compounds with highest anticancer activity are those containing copper(II) and platinum(II) as metal center (Fernandes et al. 2015; Moreira et al. 2019). Aiming to

advance in this field, we are describing herein the evaluation of anticancer activity of three copper(II) complexes against five human tumoral cell lines (THP-1, U937, Molt-4, Colo-205, NCI-H460) and normal cells (PBMC). All the copper(II) complexes were synthesized with tetradentate ligands and the main difference is the diamine backbone (ethanediamine, piperazine, homopiperazine). Then, our aim is to make correlations between antitumor activity and the structure presented by these complexes.

Experimental

Synthesis of ligands and complexes

The three ligands and their respective copper(II) complexes were synthesized as previously described and their structures are presented in Fig. 1 (Terra et al. 2016).

Antitumor activity

The antitumor activity was evaluated on five human cancer cell lines: THP-1 (acute monocytic leukemia cell line), U937 (histiocytic lymphoma cell line), Molt-4 (acute lymphoblastic), Colo-205 (human colon adenocarcinoma) and NCI-H460 (lung carcinoma). Normal peripheral blood cells (PBMC) were used as normal cell for comparison and determination of selectivity index (SI).

The evaluation of the cytotoxicity of the compounds included cell viability studies using the colorimetric MTT [3-(4,5-dimethyl-2-thihazyl)-2,5-diphenyl-2H-tetrazoliumbromide] assay. The cells were plated (approximately 1×10^6 cells) in 96 multiwell plates and treated with water solution of different concentrations of copper(II) complexes, their respective ligands and the metallic salt (CuCl$_2$·2H$_2$O), for 36 h in DMEM-F12 medium (Gibco, BRL). Cisplatin solution was prepared in DMSO.

To evaluate the cell cycle arrest the cells were plated at 1×10^6 cells cm^{-3} in 24 multiwell plates and treated with complex (3) and cisplatin for 30 h in DMEM-F12 medium (Gibco, BRL). After, the incubated cells were fixed in 70% ethanol at 4 °C for 30 min. Cells were stained with propidium iodide (PI) for 2 h in darkness. The DNA content was measured by flow cytometer (FACS Calibur-BD Sciences) and cell cycle distribution was analyzed by WinMDI version 2.9 software. The proportions of cells in G0/G1, S, and G2/M phases were represented as DNA histograms. Apoptotic cells with hypodiploid DNA content were measured by quantifying the sub-G1 peak in the cell cycle pattern.

Apoptosis was detected by using Annexin V-FITC Apoptosis Detection Kit. After incubation, NCI-H460 cells were washed twice with phosphate buffered saline (PBS) and incubated in 500 mm^3 of binding buffer (100 mmol dm^{-3} HEPES/NaOH, pH 7.5, 1.4 mol dm^{-3} NaCl and 25 mmol dm^{-3} CaCl$_2$). To each sample, 5 mm^3 of Annexin V-FITC and 10 mm^3 of PI were added. Samples were incubated at room temperature for 10 min protected from light. Cell fluorescence was determined immediately with a flow cytometer (FACS Calibur-BD Sciences). The result was determined by recording 10,000 events per sample.

The mitochondrial membrane potential ($\Delta\Psi$m) of NCI-H460 (1×10^6 cells cm^{-3}) treated with complex (3) and cisplatin during 30 h was evaluated using JC-1 stain (Morcelli et al. 2016a, b). After the elapsed time, cell suspension was transferred to a sterile tube and pelleted ($400 \times g$, for 7 min, at room temperature).
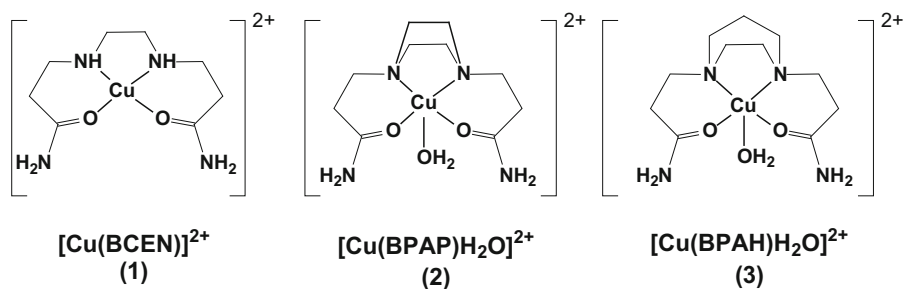

Fig. 1 Structure of copper(II) complexes

Cells were stained with JC-1 dye (25 μg cm^{-3}) and incubate at 37 °C in a 5% CO$_2$ incubator for 15 min. The mitochondria transmembrane potential (ΔΨm) was measured by flow cytometer (FACS Calibur) and was analyzed by WinMDI version 2.9 software.

For transmission electron microscopy (TEM) analyses, U937 cells were cultured at 1×10^6 cells cm^{-3} in tissue culture bottles (25 cm^2) for 12 h. The cells were incubated with different concentrations of complex (3) and cisplatin for 4 and 8 h. The cells suspension was centrifuged at $100 \times g$ for 10 min and washed three times with phosphate-buffered saline (PBS; pH 7.2). The cell pellet was fixed by 2 h in 2.5% glutaraldehyde, in 0.1 mol dm^{-3} sodium cacodylate buffer, post-fixed for 20 min in 1:1 solution osmium tetroxide (1%) and potassium ferricyanide (0.8%), dehydrated sequentially in a graded series of acetone (30–100%), and embedding in epoxy resin (Poly/Bed 812®). Resin-embedded cells were placed in a silicon mold well at 60 °C for 48 h for polymerization. The obtained blocks were sectioned and ultrathin sections (70 nm thick) were taken using an ultramicrotome Reichert Ultracut S, collected on copper grids (400 mesh), stained with uranyl acetate and lead citrate, and observed in a transmission electron microscope, TEM-900 (Zeiss, Germany) (Morcelli et al. 2016a, b).

Results and discussion

Synthesis and characterization

The ligands were synthesized through the reaction between acrylamide and different diamine units (ethylenediamine for BCEN, piperazine for BPAP and homopiperazine for BPAH) resulting in tetradentate ligands showing N$_2$O$_2$ coordination environment (Terra et al. 2016). Reactions with copper(II) chloride resulted in mononuclear copper(II) complexes (Fig. 1). The monocrystal X-ray data revealed that the complex (1) shows a square planar geometry. On the other hand, complexes (2) and (3) present distorted square pyramidal structures, in which the tetradentate ligands occupy the basal plane. The apical position in complexes (2) and (3) is occupied by a water molecule. We have shown previously that these complexes showed similar superoxide dismutase activity (Terra et al. 2016). The samples employed in this study were characterized by infrared and

elemental analyses and the data are in agreement with those previously reported (Terra et al. 2016).

Assessment of cell viability by MTT assay

In this work, the cytotoxic activity of three mononuclear copper(II) complexes was studied on five neoplastic cell lines; three of them are blood cell lines (Molt-4, U937 and THP-1) and two are solid tumors (NCI-H460 and Colo-205). In addition, tests were performed employing normal cells (peripheral blood cell line—PBMC). Control experiments using cisplatin were also carried out.

In order to obtain a more effective comparison, the results of cell viability analysis by the MTT metabolization method were converted to a 50% cytotoxicity index (IC$_{50}$), the minimum concentration capable of damaging and/or cause cell death of 50% of the cells in each analysis, which are presented in Table 1.

The IC$_{50}$ results indicate that all ligands and the copper salt (CuCl$_2$·2H$_2$O) used up to a concentration of 200 μmol dm^{-3} did not show cytotoxic activity against the cancer cell lines. However, the complexation of these ligands with copper(II) resulted in compounds that promote the reduction of cell viability of at least two neoplastic cell lines tested: Colo-205 (human colon adenocarcinoma) and NCI-H460 (lung carcinoma). This fact indicates that the complexation reactions are fundamental to potentiate the antitumor activity of the metallic center and the ligands used.

The copper(II) complexes under study presented cytotoxic activity only on solid tumor lines (NCI-H460 and Colo-205). The best result was obtained with complex (3) on lung cancer cells (NCI-H460). All the three copper complexes studied showed better activity than cisplatin (200 ± 1 μmol dm^{-3}) on this cancer cell, in the order (3) > (2) > (1) (IC$_{50}$ = 58, 71, 100 μmol dm^{-3}, respectively).

In our model, the IC$_{50}$ of cisplatin against NCI-H460 cells use to be high (Maciel et al. 2020), which contrasts with data from other laboratories. For example, Ballestreri and coworkers (Ballestreri et al. 2018) have found an IC$_{50}$ for cisplatin of 0.33 μmol dm^{-3} on NCI-H460 cells by treating 3×10^4 cells during 48 h, which is similar to the data found by Riaz et al. (Riaz et al. 2019), who found IC$_{50}$ = 0.85 μmol dm^{-3} after 72 h (cell number = 4×10^5). Of relevance is that both of them have observed that cisplatin was not toxic after 24 h of

Table 1 IC_{50} results of ligands, copper(II) complexes, $CuCl_2 \cdot 2H_2O$ and Cisplatin against NCI-H460, Molt-4, U937, THP-1, Colo-205 and PBMC cell lines after 36 h of treatment

	Cell line—IC_{50} ($\mu mol\ dm^{-3}$)						SI^a
	NCI-H460	Molt-04	U937	THP-1	Colo-205	PBMC	
Cisplatin	200 ± 1	21 ± 1	16 ± 1	12 ± 1	37 ± 1	38 ± 1[b]	0.19
$CuCl_2 \cdot 2H_2O$	> 200	> 200	> 200	> 200	> 200	–	
Ligand BCEN	> 200	> 200	> 200	> 200	> 200	–	
Ligand BPAP	> 200	> 200	> 200	> 200	> 200	–	
Ligand BPAH	> 200	> 200	> 200	> 200	> 200	–	
(1)	100 ± 2	> 200	184 ± 2	> 200	98 ± 2	> 200	> 2.0
(2)	71 ± 2	> 200	> 200	> 200	93 ± 2	> 200	> 2.8
(3)	58 ± 2	> 200	> 200	> 200	79 ± 2	> 200	> 3.4

[a]SI = Selectivity Index for NCI-H460; SI = IC_{50} for non-tumor human line (PBMC)/IC_{50} for tumor cell line (NCI-H460) (Bergamini et al. 2019)

[b]Morcelli et al. (2016a, b)

incubation. A toxic effect was observed only after 48 h. In contrast, Ferri et al. (2013) found EC_{50} = 78.3 $\mu mol\ dm^{-3}$ (3.5×10^4 cells), which is significantly higher than the data described by Ballestreri and Riaz (Ballestreri et al. 2018; Riaz et al. 2019). This difference may be related to the solvent employed to prepare the cisplatin solution. Cisplatin was solubilized in water by Riaz and in DMSO by Ferri. In this way, Hall and coworkers have pointed out that cisplatin and other platin based drugs decrease their cytotoxicity when dissolved in DMSO (Hall et al. 2014). Thus, the high IC_{50} presented by cisplatin in our study may be related to its solubilization in DMSO, the shorter treatment time (36 h) and the larger cell amount that we employed in the study. Of relevance is that cisplatin showed appreciable activity on the other cancer cells under the same conditions.

It is important to note that complexes (1), (2) and (3) were less cytotoxic on normal cells than cisplatin. Interestingly, this same order is related to the antioxidant properties (SOD-like activity) of the compounds that we have described previously (Terra et al. 2016). It has been reported recently that compounds with antioxidant activity can impair the grow and the metastasis of tumor cells (Guerreiro et al. 2020).

It was observed during the tests that NCI-H460 and Colo-205 cell lines lose their adherence capacity when treated with these compounds at 50, 100 and 200 $\mu mol\ dm^{-3}$ after 36 h of treatment. Hence, the antitumor activity of these compounds may be

associated with the adhesion mechanisms of the cells. Complex (3), which presents the larger diamine backbone (homopiperazine), showed the best antitumor activity and selectivity index for NCI-H460 (SI > 3.4), which is at least eighteen times higher than cisplatin (SI > 0.19) for this type of cancer cell.

Since complex (3) presented promisor antiproliferative effect and selectivity against NCI-H460 cell line, high water solubility and low cytotoxicity against normal peripheral blood cells (PBMC), this compound was selected to perform further investigations. Therefore, the interaction between complex (3) and NCI-H460 cell line was monitored via cell cycle analysis (Sub-G1), annexin V and propidium iodide (PI) staining, mitochondrial membrane potential ($\Delta\psi m$) analysis and transmission electron microscopy (TEM) in order to detect any morphological alterations in the NCI-H460 cell line after the treatment.

Apoptosis evaluation by Sub-G1 cell population analysis by flow cytometry

To evaluate the type of cell death induced by complex (3) on NCI-H460 tumor cells, propidium iodide (PI) labeling analysis was performed to quantify the cell DNA content after extravasation of the genetic material from the cell. Results are shown in Fig. 2. Cell cycle analysis (Sub-G1) by flow cytometry quantifies the DNA content in each phase of this cycle. This fact comes from the different amounts of
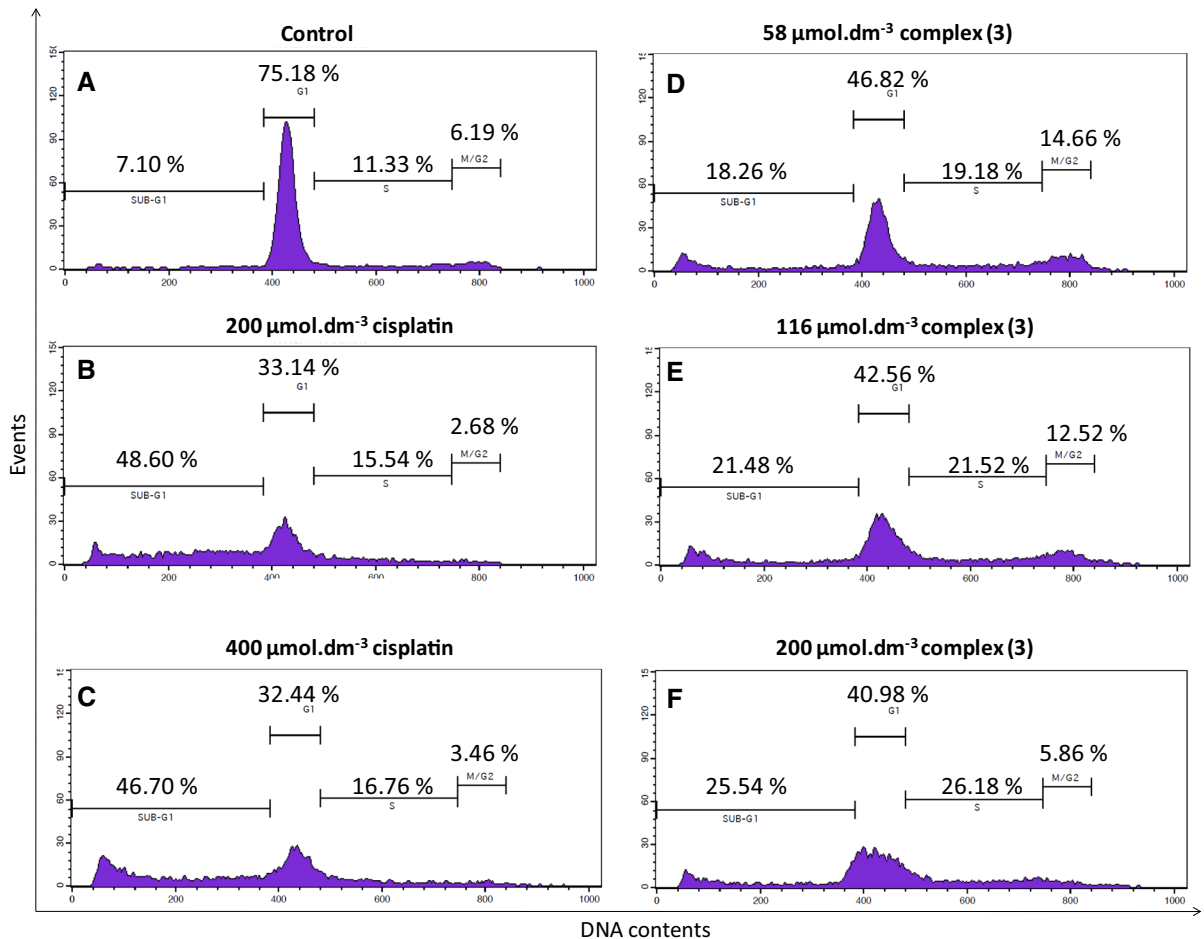
Fig. 2 Cell cycle analysis by flow cytometry. NCI-H460 was stained with propidium iodide (PI) after 30 h of incubation. Cells with hypodiploid DNA content were measured by quantifying the Sub-G1 peak in the cell cycle pattern. Each experiment per sample was determined by recording 10,000 events. **a** NCI-H460 Control cells, **b** NCI-H460 cells after treatment at the concentration of 200 μmol dm^{-3} of cisplatin; **c** NCI-H460 cells after treatment at the concentration of 400 μmol dm^{-3} of cisplatin; **d** NCI-H460 cells after treatment at the concentration of 58 μmol dm^{-3} of complex (**3**); **e** NCI-H460 cells after treatment at the concentration of 116 μmol dm^{-3} of complex (**3**); **f** NCI-H460 cells after treatment at the concentration of 200 μmol dm^{-3} of complex (**3**)

DNA in each of the stages of cell division by mitosis. The technique of cell cycle evaluation by flow cytometry is based on the interleaving of propidium iodide with DNA after disruption of the cell and nuclear membranes, forming clusters that fluoresce in the red region and are then detected by flow cytometry. In later stages of apoptosis, the DNA content is cleaved into fragments, which are quantified and appear in a region of the histogram called Sub-G1 (Gong et al. 1994). The increase of population in this region corresponds to the cells whose DNA was cleaved by nucleases, which were activated by the apoptosis processes (Morcelli et al. 2016a, b).

Cell cycle analysis indicated that both cisplatin and complex (**3**) lead to a reduction of cells in G1. From these data it can be seen that treatments with cisplatin at 200 and 400 μmol dm^{-3} result in very similar amounts of DNA in the Sub-G1 region (49% and 47%, respectively) (Fig. 2b, c). In a similar experiment employing complex (**3**) and cisplatin, both at concentration of 200 μmol dm^{-3} (Fig. 2b, f), percentages of 26% and 49% of cells in Sub-G1 were observed. It was also observed that increasing the concentration of complex (**3**) from one to twice the IC$_{50}$ does not significantly affect the amount of cells in Sub-G1 (21 and 26%, respectively) as shown in Fig. 2d, e. This

result was slightly smaller than that reported by Maciel et al. (2020) for the complex [Cu(L1)Cl]Cl·2H$_2$O, where L1 = 1-[2-hydroxybenzyl(2-pyridyl-methyl)amino]-3-(1-naphthyloxy)-2-propanol, which showed 32% of NCI-H460 cells in sub-G1 region when twice the IC$_{50}$ concentration was used. The data indicate that complex (**3**) and cisplatin induces cell death by apoptosis, what are in agreement with other studies carried out by us in this work.

NCI-H460 cells undergo apoptosis after treatment by copper(II) complex

To confirm the type of cell death, annexin V and propidium iodide (PI) labeling techniques were used. The results are shown in Fig. 3 for NCI-H460 cells after treatment with concentrations equivalent to one and twofolds the IC$_{50}$ value and 200 μmol dm^{-3} of the

[Cu(BPAH)H$_2$O]Cl$_2$, (**3**), complex. In the dot plots figure, the lower left quadrant indicates the presence of cells that were not marked by annexin V or propidium iodide, so these cells are considered viable cells. The lower right quadrant indicates cells marked with annexin V only, which is typical of cells undergoing apoptosis. In contrast, the upper left quadrant indicates cells that were labeled with propidium iodide only, related to cell death by necrosis. The existence of double marked in the right upper quadrant indicates cell death due to apoptosis and lately staining by propidium iodide, secondary necrosis (Moreira et al. 2019).

In the assay performed after 30 h of incubation, the Annexin V/PI graph shows a percentage of 92% of living cells for the control, indicating that the cells were properly cultured (Fig. 3a). Employing the IC$_{50}$ concentration of complex (**3**), 28% of the cells were in
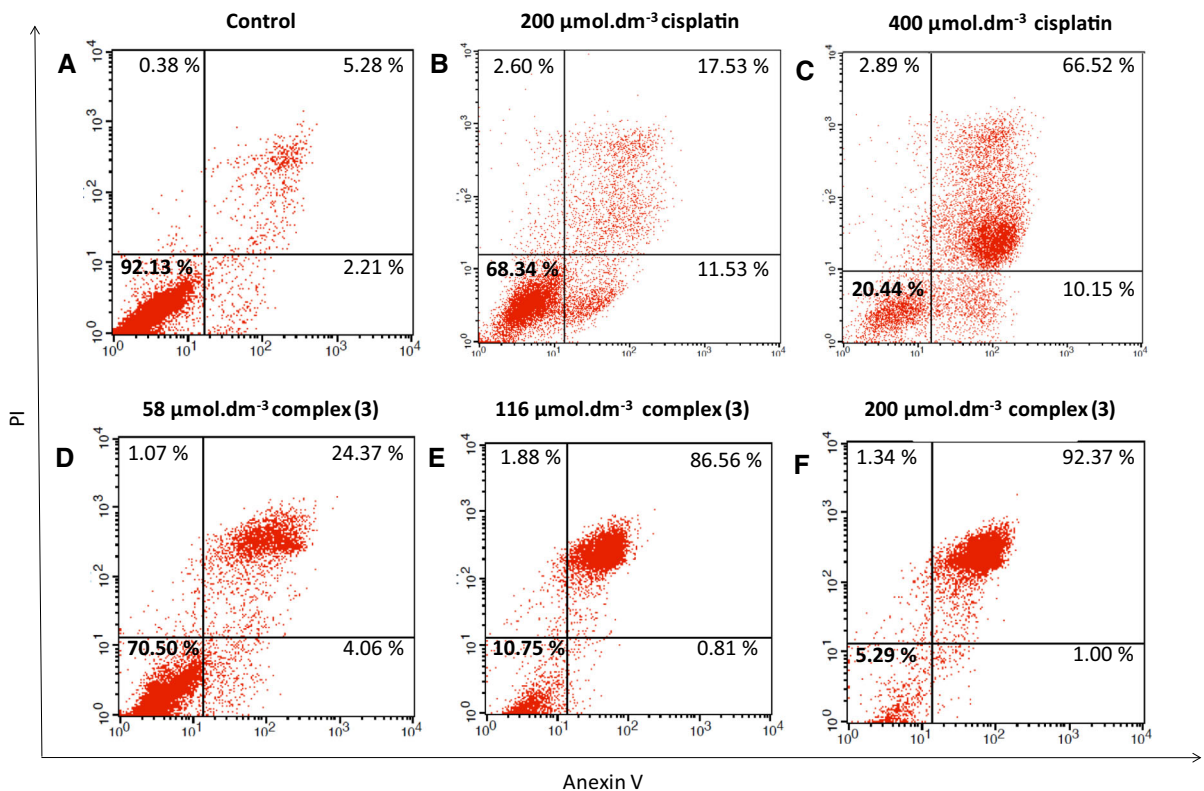

Fig. 3 Annexin V-FITC/PI staining detected apoptosis induced by complex (**3**) and cisplatin, in NCI-H460 cells, after treatment for 30 h. **a** Control cells; **b** NCI-H460 cells after treatment at the concentration of 200 μmol dm^{-3} of cisplatin; **c** NCI-H460 cells after treatment at the concentration of 400 μmol dm^{-3} of cisplatin; **d** NCI-H460 cells after treatment at the concentration of 58 μmol dm^{-3} of complex (**3**); **e** NCI-H460 cells after treatment at the concentration of 116 μmol dm^{-3} of complex (**3**); **f** NCI-H460 cells after treatment at the concentration of 200 μmol . dm^{-3} of complex (**3**); The data are presented in dot plots depicting annexinV/FITC versus PI staining. The percentage of cells in each quadrant is presented
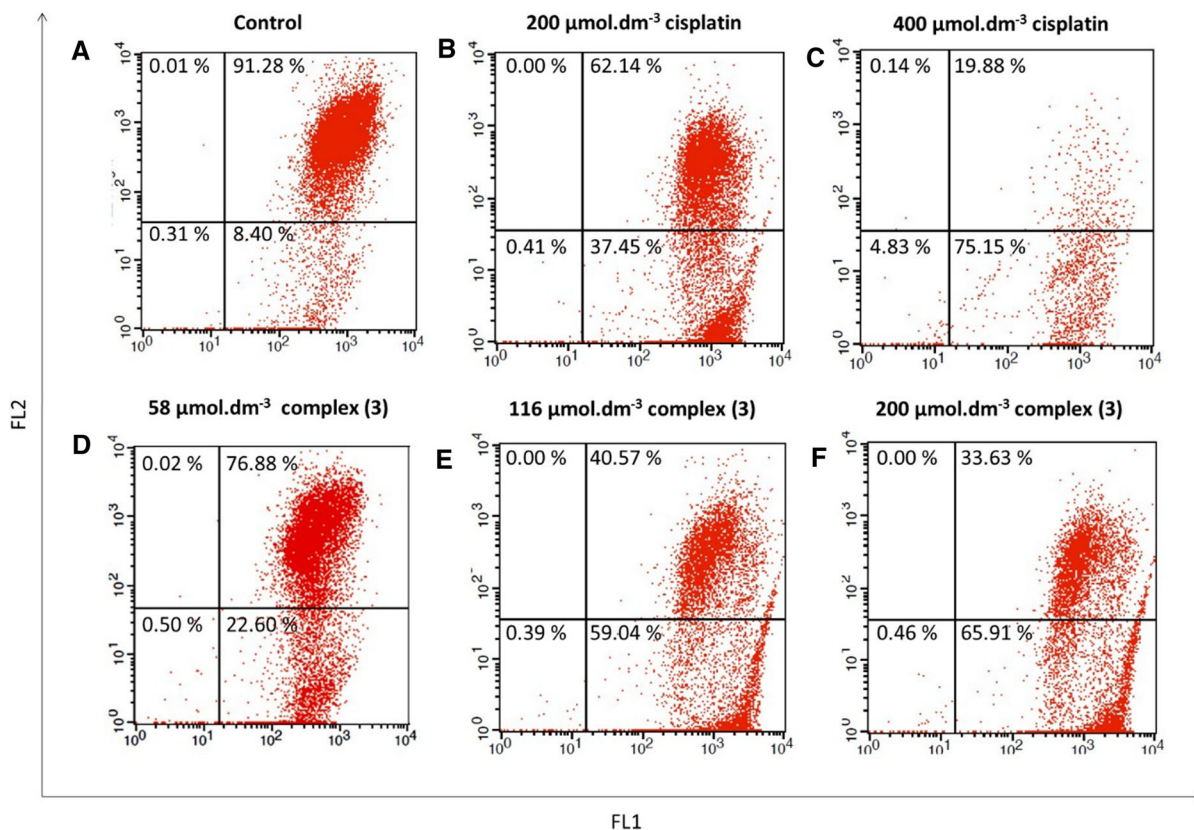
Fig. 4 Mitochondrial transmembrane potential ($\Delta\Psi$m) assay. NCI-H460 cells were incubated with complex (**3**) and cisplatin for 30 h. After being stained with JC-1, cells were analyzed by flow cytometry. Quadrant Q2 (up right)—mitochondria containing red JC-1 aggregates in healthy cells are detected in the FL2 channel. Quadrant Q4 (bottom right)—green JC-1 monomers in apoptotic cells are detectable in the FITC channel (FL1) and express a loss of $\Delta\Psi$m. **a** Control cells; **b** NCI-H460 cells after treatment at the concentration of 200 µmol dm^{-3} of cisplatin; **c** NCI-H460 cells after treatment at the concentration of 400 µmol dm^{-3} of cisplatin; **d** NCI-H460 cells after treatment at the concentration of 58 µmol dm^{-3} of complex (**3**); **e** NCI-H460 cells after treatment at the concentration of 116 µmol dm^{-3} of complex (**3**); **f** NCI-H460 cells after treatment at the concentration of 200 µmol dm^{-3} of complex (**3**)

apoptosis (Fig. 3d), whereas treatment with $2 \times IC_{50}$ led to a percentage of 87% (Fig. 3e). This value is around 10% smaller than the one (98%) observed for the complex [Cu(L1)Cl]Cl·2H$_2$O, reported by Maciel et al. (2020). Treatment employing 200 µmol dm^{-3} of complex (**3**) resulted in 93% of cell death by apoptosis (Fig. 3f). The data observed for this copper(II) complex also showed that it has higher activity than cisplatin, which promoted only 29% of cell death by apoptosis at this concentration (200 µmol dm^{-3}) (Fig. 3b) and 76% when cells of the same type were treated with a concentration equal to twice the IC_{50} (Fig. 3c).

Analysis of mitochondrial membrane potential ($\Delta\Psi$m)

In addition to the Annexin V/PI assay, the staining method of JC-1 (5,5′,6,6′-tetrachloro-1,1′,3,3′-tetraethylbenzimidazolylcarbocyanine iodide) was performed, which indicates alterations in the mitochondrial membrane potential. When there is loss of mitochondrial function, cells begin the process of cell death by apoptosis (Gillan et al. 2005). The technique is based on JC-1 concentration difference inside the cells. When its concentration becomes high in the mitochondrial matrix, JC-1 form aggregates and emits red fluorescence, indicating that the mitochondrial membrane is not damaged. In cells where
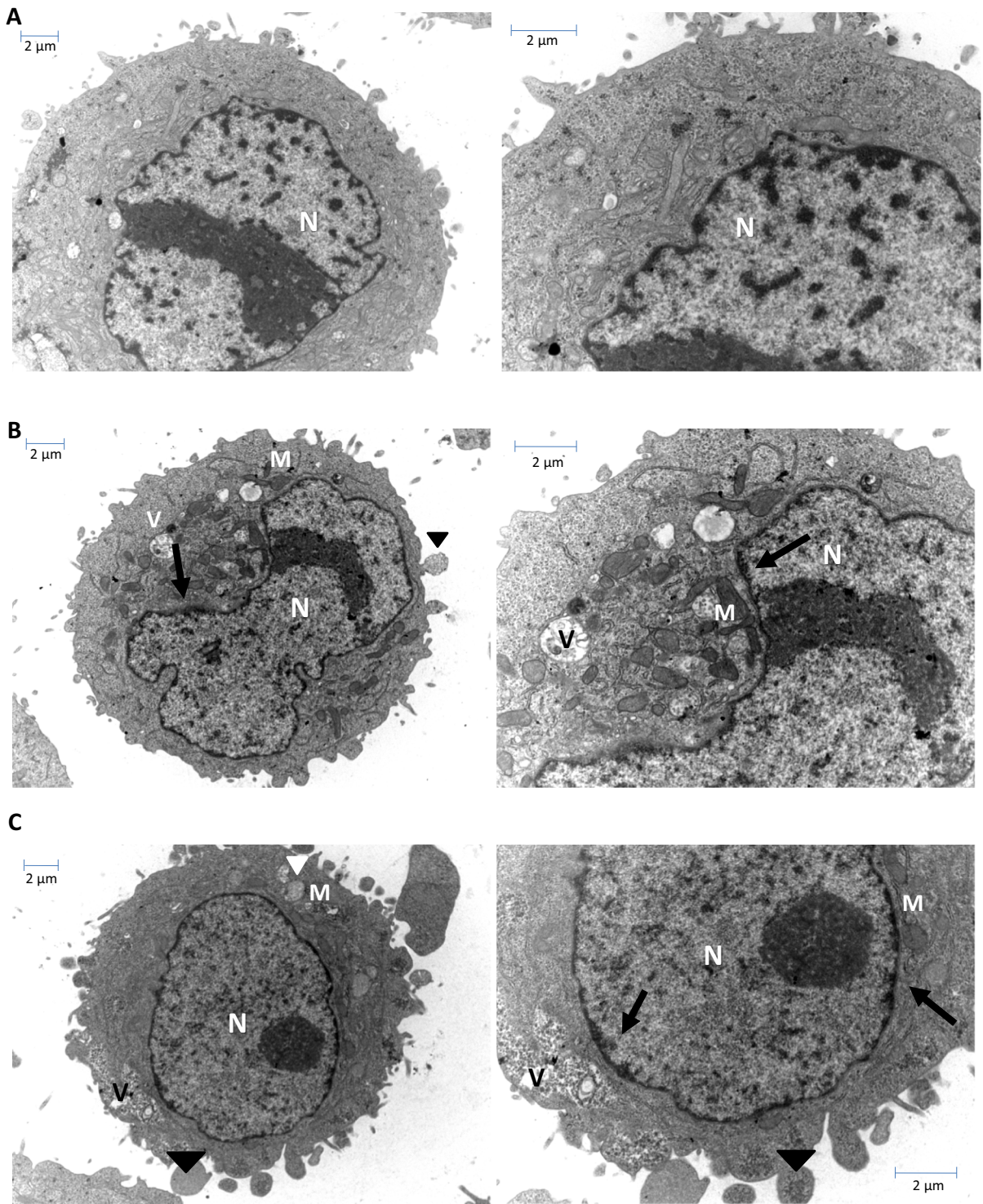
Fig. 5 Transmission electron microscopy of the NCI-H460 lung carcinoma strain. **a** Control cells, **b** NCI-H460 cells incubated with 58 µmol dm^{-3} of complex (**3**) for 4 h, **c** NCI-H460 cell line incubated with 58 µmol dm^{-3} of complex (**3**) for 8 h. M = Mitochondria; V = Vacuoles and N = Nucleus. Chromatin condensation is indicated by the black arrow and apoptotic bodies are indicated by the black triangles
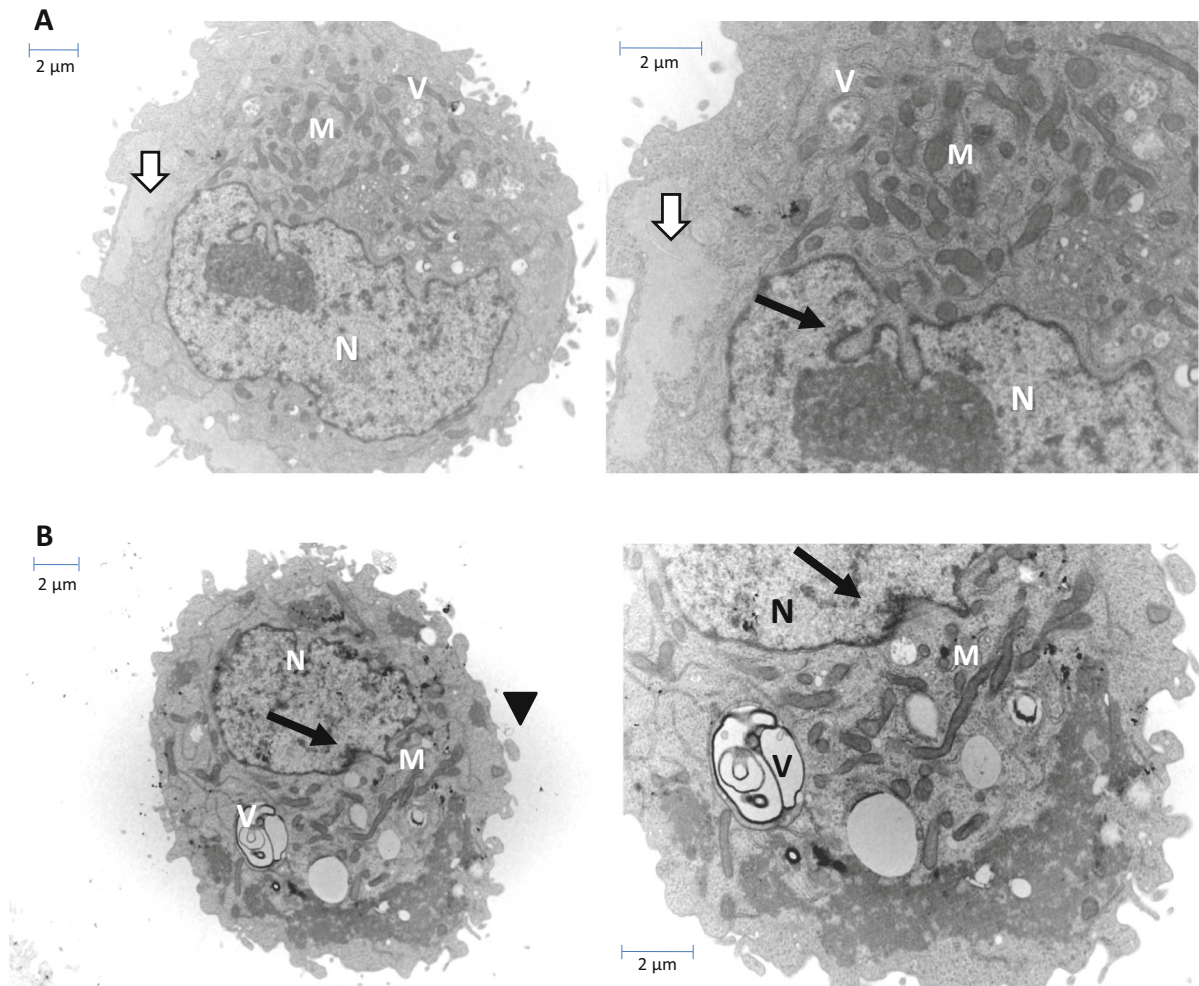
Fig. 6 Transmission electron microscopy of human lung cancer cells. **a** NCI-H460 cell line incubated with 116 μmol dm^{-3} of complex (**3**) for 4 h. **b** NCI-H460 cell line incubated with 116 μmol dm^{-3} of complex (**3**) for 8 h. M = Mitochondria;

V = Vacuoles and N = Nucleus. Chromatin condensation is indicated by the black arrow, apoptotic bodies are indicated by the black triangles and a reduction in some glycogen stores is indicated by the white arrow

mitochondrial membrane potential collapse has occurred, JC-1 aggregate formation does not occur and the cells have green-fluorescence cytoplasm (Smiley et al. 1991).

Figure 4 shows the results for NCI-H460 cells treated with a concentration equivalent to one and two fold the IC$_{50}$ value of the complex (**3**) and cisplatin, plus a concentration of 200 μmol dm^{-3} of the complex (**3**).

The data for complex (**3**) indicate that it has a smaller reduction of mitochondrial activity compared to cisplatin. When cells were treated with a cisplatin concentration equal to the IC$_{50}$ value (Fig. 4b), 37% of the cells underwent changes in the mitochondrial

membrane potential and 75% when cells were treated with two folds IC$_{50}$ (Fig. 4c), being observed that the values are very close to the data presented by the annexin V/PI technique. When a concentration equivalent to IC$_{50}$ of the complex (**3**) was used, around 23% of the cells had lost their mitochondrial membrane potential (Fig. 4d). This value reaches 59% when treated with twice the IC$_{50}$ value (Fig. 4e) and 66% with 200 μmol dm^{-3} of the complex (**3**) (Fig. 4f). These data suggest that the cytotoxic performance of complex (**3**) is not fully related to mitochondrial activity, since there are a higher percentage of apoptotic cells than cells with damaged mitochondria. Similar to our complex several metal complexes
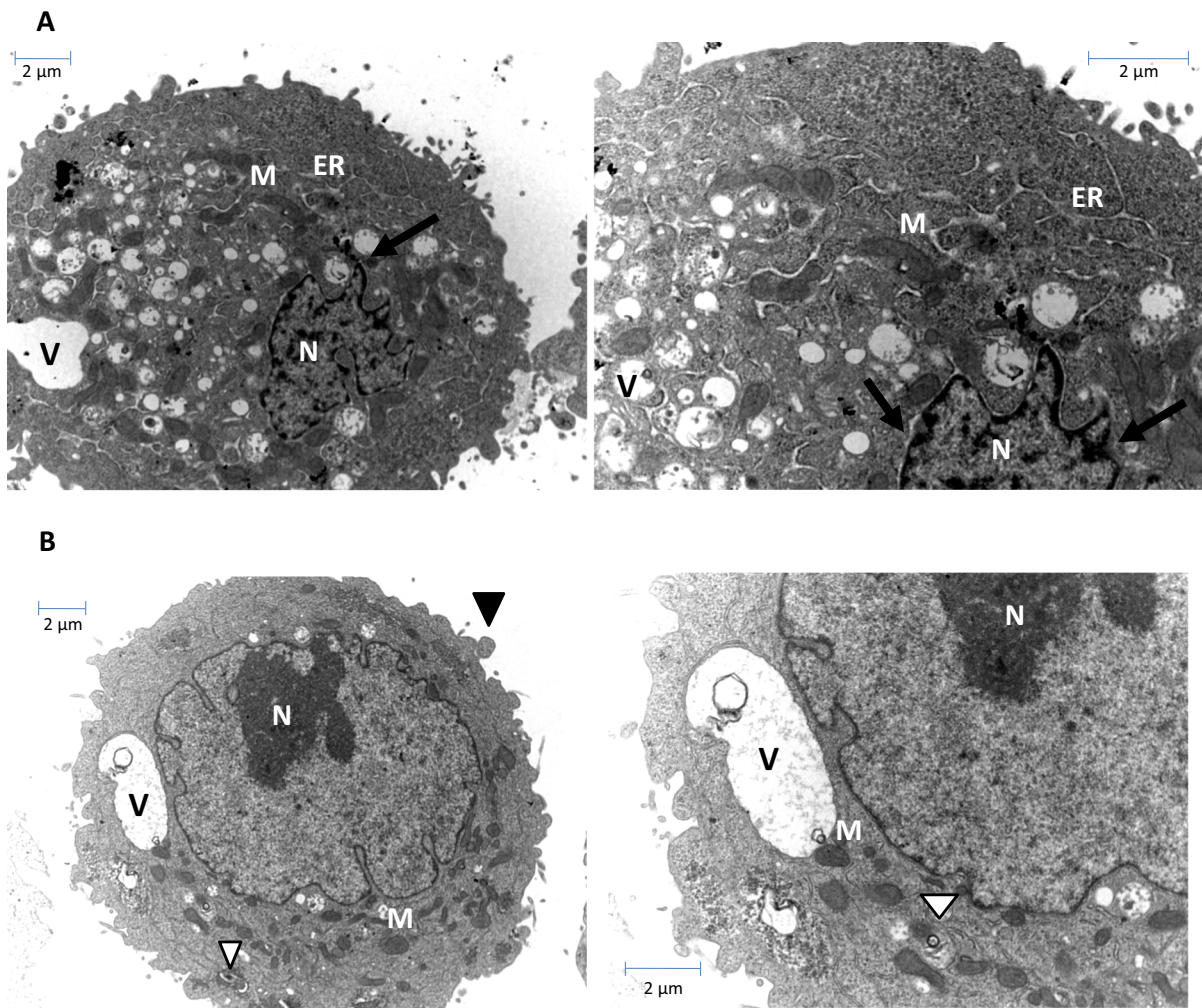
Fig. 7 Transmission electron microscopy of human lung cancer cells. **a** NCI-H460 cells incubated with 200 μmol dm^{-3} of complex (**3**) for 4 h. **b** NCI-H460 cell line incubated with 200 μmol dm^{-3} of complex (**3**) for 8 h. M = Mitochondria; ER = Endoplasmic Reticulum; V = Vacuoles and N = Nucleus. Chromatin condensation is indicated by the black arrow, apoptotic bodies are indicated by the black triangles and empty mitochondria matrix is indicated by the white triangle

induce apoptosis through mitochondrial pathway (Borges et al. 2016; Erxleben 2018; Fernandes et al. 2015; Horn Jr. et al. 2013; Marín-Hernández et al. 2003; Morcelli et al. 2016a, b). Most of them interact to DNA, at least in vitro and impair the repair process triggering the nuclear apoptosis signaling.

Analysis of cell morphology by transmission electron microscopy (TEM)

Transmission electron microscopy (TEM) was used in this work to ascertain the morphological changes presented by NCI-H460 tumor cells when treated with different concentrations (58 μmol dm^{-3}, 116 μmol dm^{-3} and 200 μmol dm^{-3}) of the complex (**3**) and incubated for 4 and 8 h. After this period, the treated and untreated NCI-H460 cells were processed and observed by transmission electron microscopy (Figs. 5, 6 and 7).

The cell morphology of NCI-H460 lung carcinoma prior the treatment is shown in Fig. 5a. NCI-H460 cells from the control group present a homogenous cytoplasm, with regular organelles (mitochondria and endoplasmic reticulum) and low amount of vacuole-like structures, indicating good cell status.

The transmission electron microscopy presented in Figs. 5, 6 and 7 revealed significant morphological changes in NCI-H460 cells after treatment with complex (**3**). In all cases, chromatin condensation was observed in the nuclear periphery [black arrow] (Figs. 5c, 6a, b and 7a), which is indicative of cell death by apoptosis. In all treatments, changes in mitochondrial structures were also observed, such as swelling and enlargement of these organelles (M). These changes are consistent with the JC-1 data presented above, indicating that mitochondria participate in the apoptosis cell death process. Furthermore, vacuolization of different organelles were observed, and some of them performed engulfing processes (V and white triangle for empty mitochondria matrix, Fig. 7b). In some cases, apoptotic bodies aggregated to cell membranes were also found (black triangle), mainly in the analyzes performed after incubation for 8 h (Figs. 5b, c and 6b). At higher concentrations (200 μmol dm^{-3}) there was a slight widening in the structures of the endoplasmic reticulum (ER), suggesting the participation of this organelle in the apoptotic cell death process, as stated previously by Maciel et al. (2020). Finally, a reduction in some glycogen stores was also observed (white arrow), Fig. 6a, probably due to an increase in cellular metabolism, which aims the recovery of damaged organelles.

Conclusion

The cytotoxic activity of three mononuclear copper(II) complexes were evaluated on non-adherent (Molt-04, U937, THP-1) and adherent (NCI-H460, Colo-205) tumor cells. All the complexes presented activity only on the adherent cells and the best result was shown by the complex $[Cu(BPAH)(H_2O)]^{2+}$, (**3**), on lung NCI-H460 cell line cancer, presenting an IC$_{50}$ almost four-fold lower than cisplatin. Furthermore, this complex was not cytotoxic against PBMC, presenting high selectivity toward NCI-H460 (SI > 3.4).

Further studies showed that (**3**) induces apoptosis in the NCI-H460 cell line with the impairment of the mitochondria, endoplasmic reticulum and other organelles, which was confirmed by mitochondrial transmembrane potential analysis and TEM investigations. Considering the structure and antioxidant properties of the three compounds reported in this study, we can state that the relevant antitumor activity exhibited by complex (**3**) should be related to the presence of the larger diamine unit (homopiperazine) and the antioxidant activity, which was previously described by us.

Declarations

Conflict of interest The authors state that there are no conflict of interests.

References

Adams MN, Ashton NW, Paquet N, O'Byrne K, Richard DJ (2014) Mechanisms of cisplatin resistance: DNA repair and cellular implications. Adv Drug Resistance Res

Ahmad A, Ahsan H (2020) Ras-mediated activation of NF-κB and DNA damage response in carcinogenesis. Cancer Invest. https://doi.org/10.1080/07357907.2020.1721523

Arffman M, Manderbacka K, Suvisaari J, Koivunen J, Lumme S, Keskimäki I, Ahlgren-Rimpiläinen A, Pukkala E (2018) The impact of severe mental illness on mortality of lung cancer in Finland in 1990–2014. Eur J Pub Health. https://doi.org/10.1093/eurpub/cky214.254

Babak MV, Ang WH (2018) Multinuclear organometallic ruthenium-arene complexes for cancer therapy. Metallo-Drugs. https://doi.org/10.1515/9783110470734-006

Ballestreri É, Simon D, Souza AP, Grott CS, Nabinger DD, Dihl RR, Grivicich I (2018) Resistance mechanism to cisplatin in NCI-H460 non-small cell lung cancer cell line: investigating apoptosis, autophagy, and cytogenetic damage. Cancer Drug Resistance 1:72–81

Bergamini FRG, Nunes JHB, de Carvalho MA, Ribeiro MA, de Paiva PP, Banzato TP, Ruiz ALTG, de Carvalho JE, Lustri WR, Martins DOTA, da Costa Ferreira AM, Corbi PP (2019) Polynuclear copper(II) complexes with nalidixic acid hydrazones: Antiproliferative activity and selectivity assessment over a panel of tumor cells. Inorg Chim Acta 484:491–502. https://doi.org/10.1016/j.ica.2018.09.084

Borges LJH, Bull ÉS, Fernandes C, Horn A, Azeredo NF, Resende JALC, Freitas WR, Carvalho ECQ, Lemos LS, Jerdy H, Kanashiro MM (2016) In vitro and in vivo studies of the antineoplastic activity of copper (II) compounds against human leukemia THP-1 and murine melanoma B16–F10 cell lines. Eur J Med Chem. https://doi.org/10.1016/j.ejmech.2016.07.018

Bray F, Ferlay J, Soerjomataram I, Siegel RL, Torre LA, Jemal A (2018) Global cancer statistics 2018: GLOBOCAN estimates of incidence and mortality worldwide for 36 cancers in 185 countries. CA. https://doi.org/10.3322/caac.21492

Cancer. (n.d.). Retrieved April 7, 2020, from https://www.who.int/news-room/fact-sheets/detail/cancer

Chitambar CR (2018) Gallium complexes as anticancer drugs. Metallo-Drugs. https://doi.org/10.1515/9783110470734-010

Cini M, Bradshaw TD, Woodward S (2017) Using titanium complexes to defeat cancer: the view from the shoulders of titans. Chem Soc Rev. https://doi.org/10.1039/c6cs00860g

Comba P, Gahan LR, Hanson GR, Mereacre V, Noble CJ, Powell AK, Prisecaru I, Schenk G, Zajaczkowski-Fischer M (2012) Monoesterase activity of a purple acid phosphatase mimic with a cyclam platform. Chem Eur J 18:1700–1710. https://doi.org/10.1002/chem.201100229

Cong L, Feng W, Yao Z, Zhou X, Xiao W (2020) Deep learning model as a new trend in computer-aided diagnosis of tumor pathology for lung cancer. J Cancer 11(12):3615–3622. https://doi.org/10.7150/jca.43268

Crans DC, Yang L, Haase A, Yang X (2018) Health benefits of vanadium and its potential as an anticancer agent. Metallo-Drugs. https://doi.org/10.1515/9783110470734-009

Denoyer D, Clatworthy SAS, Cater MA (2018) Copper complexes in cancer therapy. Metallo-Drugs. https://doi.org/10.1515/9783110470734-016

Erxleben A (2018) Mitochondria-targeting anticancer metal complexes. Curr Med Chem. https://doi.org/10.2174/0929867325666180307112029

Fernandes C, Parrilha GL, Lessa JA, Santiago LJM, Kanashiro MM, Boniolo FS, Bortoluzzi AJ, Vugman NV, Herbst MH, Horn A Jr (2006) Synthesis, crystal structure, nuclease and in vitro antitumor activities of a new mononuclear copper(II) complex containing a tripodal N₃O ligand. Inorg Chim Acta. https://doi.org/10.1016/j.ica.2006.04.007

Fernandes C, Horn A, Lopes BF, Bull ES, Azeredo NFB, Kanashiro MM, Borges FV, Bortoluzzi AJ, Szpoganicz B, Pires AB, Franco RWA, Almeida JCDA, Maciel LLF, Resende JALC, Schenk G (2015) Induction of apoptosis in leukemia cell lines by new copper(II) complexes containing naphthyl groups via interaction with death receptors. J Inorg Biochem. https://doi.org/10.1016/j.jinorgbio.2015.09.014

Ferri N, Cazzaniga S, Mazzarella L, Curigliano G, Lucchini G, Zerla D, Gandolfi R, Facchetti G, Pellizzoni M, Rimoldi I (2013) Cytotoxic effect of (1-methyl-1H-imidazol-2-yl)-methanamine and its derivatives in PtII complexes on human carcinoma cell lines: a comparative study with cisplatin. Bioorg Med Chem. https://doi.org/10.1016/j.bmc.2013.01.063

Florea AM, Büsselberg D (2011) Cisplatin as an anti-tumor drug: Cellular mechanisms of activity, drug resistance and induced side effects. Cancers. https://doi.org/10.3390/cancers3011351

Gallagher WM, Cairney M, Schott B, Roninson IB, Brown R (1997) Identification of p53 genetic suppressor elements which confer resistance to cisplatin. Oncogene. https://doi.org/10.1038/sj.onc.1200813

Gillan L, Evans G, Maxwell WMC (2005) Flow cytometric evaluation of sperm parameters in relation to fertility potential. Theriogenology. https://doi.org/10.1016/j.theriogenology.2004.09.024

Gong JP, Traganos F, Darzynkiewicz Z (1994) A selective procedure for DNA extraction from apoptotic cells applicable for gel electrophoresis and flow cytometry. Anal Biochem. https://doi.org/10.1006/abio.1994.1184

Guerreiro JF, Gomes MAGB, Pagliari F, Jansen J, Marafioti MG, Nistico C, Hanley R, Costa RO, Ferreira SS, Mendes F, Fernandes C, Horn A, Tirinato L, Seco J (2020) Iron and copper complexes with antioxidant activity as inhibitors of the metastatic potential of glioma cells. RSC Adv. https://doi.org/10.1039/D0RA00166J

Gutschner T, Diederichs S (2012) The hallmarks of cancer: A long non-coding RNA point of view. RNA Biol. https://doi.org/10.4161/rna.20481

Hall MD, Telma KA, Chang KE, Lee TD, Madigan JP, Lloyd JR, Goldlust IS, Hoeschele JD, Gottesman MM (2014) Say no to DMSO: dimethylsulfoxide inactivates cisplatin, carboplatin, and other platinum complexes. Can Res. https://doi.org/10.1158/0008-5472.CAN-14-0247

Horn A Jr, Fernandes C, Parrilha GL, Kanashiro MM, Borges FV, De Melo EJT, Schenk G, Terenzi H, Pich CT (2013) Highly efficient synthetic iron-dependent nucleases activate both intrinsic and extrinsic apoptotic death pathways in leukemia cancer cells. J Inorg Biochem. https://doi.org/10.1016/j.jinorgbio.2013.07.019

Huang J, Weinstein SJ, Yu K, Männistö S, Albanes D (2020) A prospective study of serum vitamin E and 28-year risk of lung cancer. J Natl Cancer Inst. https://doi.org/10.1093/jnci/djz077

Kartalou M, Essigmann JM (2001) Mechanisms of resistance to cisplatin. Mutation Res. https://doi.org/10.1016/S0027-5107(01)00141-5

Kioseoglou E, Petanidis S, Gabriel C, Salifoglou A (2015) The chemistry and biology of vanadium compounds in cancer therapeutics. Coord Chem Rev. https://doi.org/10.1016/j.ccr.2015.03.010

Lessa JA, Parrilha GL, Beraldo H (2012) Gallium complexes as new promising metallodrug candidates. Inorg Chim Acta. https://doi.org/10.1016/j.ica.2012.06.003

Maciel LLF, de Freitas WR, Bull ES, Fernandes C, Horn A, de Aquino Almeida JC, Kanashiro MM (2020) In vitro and in vivo anti-proliferative activity and ultrastructure investigations of a copper(II) complex toward human lung cancer cell NCI-H460. Journal of Inorganic Biochemistry 210: https://doi.org/10.1016/j.jinorgbio.2020.111166

Marín-Hernández A, Gracia-Mora I, Ruiz-Ramírez L, Moreno-Sánchez R (2003) Toxic effects of copper-based antineoplastic drugs (Casiopeinas®) on mitochondrial functions. Biochem Pharmacol. https://doi.org/10.1016/S0006-2952(03)00212-0

Miller KD, Nogueira L, Mariotto AB, Rowland JH, Yabroff KR, Alfano CM, Jemal A, Kramer JL, Siegel RL (2019) Cancer treatment and survivorship statistics, 2019. CA Cancer J Clin. https://doi.org/10.3322/caac.21565

Morcelli SR, Bull ÉS, Terra WS, Moreira RO, Borges FV, Kanashiro MM, Bortoluzzi AJ, Maciel LLF, Almeida JCDA, Júnior AH, Fernandes C (2016a) Synthesis, characterization and antitumoral activity of new cobalt(II)-complexes: Effect of the ligand isomerism on the biological activity of the complexes. J Inorg Biochem. https://doi.org/10.1016/j.jinorgbio.2016.05.003

Morcelli SR, Kanashiro MM, Candela DRS, Alzamora M, Horn A, Fernandes C (2016b) Synthesis, characterization and antitumoral activity of new di-iron(III) complexes

containing naphthyl groups: effect of the isomerism on the biological activity. Inorg Chem Commun. https://doi.org/10.1016/j.inoche.2016.02.016

Moreira RO, Morcelli SR, Kanashiro MM, Resende JALC, Maciel LLF, João JC, Gahan LR, Horn A, Fernandes C (2019) Modulating the antitumoral activity by the design of new platinum(II) compounds: synthesis, characterization, DFT, ultrastructure and mechanistic studies. J Inorg Biochem. https://doi.org/10.1016/j.jinorgbio.2018.12.016

Muhammad N, Guo Z (2014) Metal-based anticancer chemotherapeutic agents. Curr Opin Chem Biol. https://doi.org/10.1016/j.cbpa.2014.02.003

Pugazhendhi A, Edison TNJI, Karuppusamy I, Kathirvel B (2018) Inorganic nanoparticles: A potential cancer therapy for human welfare. Int J Pharm. https://doi.org/10.1016/j.ijpharm.2018.01.034

Riaz MA, Sak A, Erol YB, Groneberg M, Thomale J, Stuschke M (2019) Metformin enhances the radiosensitizing effect of cisplatin in non-small cell lung cancer cell lines with different cisplatin sensitivities. Sci Rep. https://doi.org/10.1038/s41598-018-38004-5

Riddell IA, Lippard SJ (2018) Cisplatin and oxaliplatin: our current understanding of their actions. Metallo-Drugs. https://doi.org/10.1515/9783110470734-001

Ruiz-Azuara L, Bastian G, Bravo-Gómez ME, Cañas RC, Flores-Alamo M, Fuentes I, Mejia C, García-Ramos JC, Serrano A (2014) Abstract CT408: phase I study of one mixed chelates copper(II) compound. Casiopeína CasIIIia with antitumor activity and its mechanism of action. https://doi.org/10.1158/1538-7445.am2014-ct408

Santini C, Pellei M, Gandin V, Porchia M, Tisato F, Marzano C (2014) Advances in copper complexes as anticancer agents. Chem Rev. https://doi.org/10.1021/cr400135x

Shi K, Li N, Yang M, Li W (2019) Identification of key genes and pathways in female lung cancer patients who never smoked by a bioinformatics analysis. J Cancer. https://doi.org/10.7150/jca.26908

Smiley ST, Reers M, Mottola-Hartshorn C, Lin M, Chen A, Smith TW, Steele GD, Chen LB (1991) Intracellular heterogeneity in mitochondrial membrane potentials revealed by a J-aggregate-forming lipophilic cation JC-1. Proc Natl Acad Sci USA. https://doi.org/10.1073/pnas.88.9.3671

Stewart DJ (2007) Mechanisms of resistance to cisplatin and carboplatin. Crit Rev Oncol Hematol. https://doi.org/10.1016/j.critrevonc.2007.02.001

Terra WS, Ferreira SS, Costa RO, Mendes L, Franco RWA, Bortoluzzi AJ, Resende JALC, Fernandes C, Horn A (2016) Evaluating the influence of the diamine unit (ethylenediamine, piperazine and homopiperazine) on the molecular structure, physical chemical properties and superoxide dismutase activity of copper complexes Dedicated to Prof. Ademir Neves on the occasion of. Inorg Chim Acta. https://doi.org/10.1016/j.ica.2016.06.024

Tshuva EY, Miller M (2018) Coordination complexes of titanium(IV) for anticancer therapy. Metallo-Drugs. https://doi.org/10.1515/9783110470734-008

Wang S, Liu Y, Feng Y, Zhang J, Swinnen J, Li Y, Ni Y (2019) A review on curability of cancers: more efforts for novel therapeutic options are needed. Cancers. https://doi.org/10.3390/cancers11111782

Wani WA, Baig U, Shreaz S, Shiekh RA, Iqbal PF, Jameel E, Ahmad A, Mohd-Setapar SH, Mushtaque M, Ting Hun L (2016) Recent advances in iron complexes as potential anticancer agents. New J Chem. https://doi.org/10.1039/c5nj01449b

Yu Z, Yan B, Gao L, Dong C, Zhong J, D'Ortenzio M, Nguyen B, Seong Lee S, Hu X, Liang F (2016) Targeted delivery of bleomycin: a comprehensive anticancer review. Curr Cancer Drug Targets. https://doi.org/10.2174/1568009616666151130213910

Zeng L, Gupta P, Chen Y, Wang E, Ji L, Chao H, Chen ZS (2017) The development of anticancer ruthenium(II) complexes: From single molecule compounds to nanomaterials. Chem Soc Rev. https://doi.org/10.1039/c7cs00195a